Journal of
Nanoscience and Nanotechnology
Vol. 8, 1–6, 2008

Hierarchical ZnO Nanostructures: Growth and Optical Properties

Ahmad Umar[1,*], A. Al. Hajry[2], S. Al-Heniti[3], and Y.-B. Hahn[1,*]

[1] *School of Semiconductor and Chemical Engineering, and BK 21, Centre for Future Energy Materials and Devices, Chonbuk National University, Jeonju, South Korea*
[2] *Department of Physics, Faculty of Science, King Khalid University, Abha, Saudi Arabia*
[3] *Department of Physics, Faculty of Science, King Abdul Aziz University, Saudi Arabia*

Growth of hierarchical ZnO nanostructures composed of ZnO nanoneedles have been achieved via simple thermal evaporation process by using metallic zinc powder in the presence of oxygen at low temperature of 460 °C on silicon substrate without the use of any kind of metal catalysts or additives. It is confirmed by detailed structural studies that the as-grown hierarchical nanostructures are single crystalline with a wurtzite hexagonal phase and nanoneedles of these structures are grown along the c-axis in the [0001] direction. The Raman-scattering analysis substantiates a wurtzite hexagonal phase with a good crystal quality for the as-grown products. Room-temperature photoluminescence (PL) exhibits a strong UV emission at 380 nm confirming the excellent optical properties of as-synthesized hierarchical structures. A plausible growth mechanism is also proposed to clearly understand the growth process of the synthesized structures.

Keywords: Hierarchical Nanostructures, ZnO, Structural Properties, Optical Properties.

RESEARCH ARTICLE

1. INTRODUCTION

Among different metal oxide semiconductor nanostructures, the II-VI semiconductor zinc oxide (ZnO) is a key engineering material on its own merits. With a wide band-gap (3.37 eV), ZnO presents itself as one of the potential and important material for the fabrication of efficient laser diodes, light emitting diodes, optical waveguides, optical switches, and so on.[1–4] Moreover, the high exciton binding energy (60 meV) makes it a promising candidate for the room-temperature ultraviolet laser diodes.[5] In addition to this, ZnO is highly applicable in various high-technological applications due to its excellent and marvelous properties such as chemical and thermal stabilities, electronic and optoelectronic properties, large saturation velocity, high-break down voltage, etc. The applications such as surface acoustic wave filters, photonic crystals, photodetectors, photodiodes, optical modulator, gas sensors, chemical and bio-sensors, varistors, solar cells, and etc. are all based on ZnO nanostructures.[6–14] As a wurtzite hexagonal phase, ZnO also possesses non-centrosymmetric structure hence exhibits a piezoelectric nature which is a cardinal property for the fabrication of electromechanical coupled sensors, actuators and transducers.[15–17] By exploring this piezoelectric properties, recently Wang discovered a nanogenerator which were able to convert the mechanical energy into electric energy.[18] Including diverse properties and vast applications, the ZnO is a material that has wide morphological diversity; hence it is believed that the ZnO is probably the richest family of nanostructures among all materials, both in structural and properties view point.[19–25]

Heretofore, variety of ZnO nanostructures have been synthesized by using numerous fabrication techniques and reported in the literature.[25–34] In addition to common 1D morphologies, some hierarchical nanoarchitectures of ZnO made by the assembly of 1D nanostructure are also reported in the literature.[35–39] Variety of hierarchical ZnO nanostructures with 6-, 4-, and 2-fold symmetries, nanobridges and nanonails were synthesized by Lao et al. using the mixed powders of ZnO, In_2O_3 and graphite by the vapor transport and condensation method at the temperature ranges between 950–1000 °C.[35–37] Nanopropeller arrays of ZnO have been synthesized by Gao et al. via two-step high-temperature solid-vapor deposition process at the temperature of 1300 °C by using the mixtures of ZnO, SnO_2 and graphite.[38] Hierarchical microbelts of ZnO nanobowlin-pin arrays were synthesized by Shen et al. via atmospheric pressure thermal evaporation process by using the mixtures of metallic zinc powder, In and/or In_2S_3 as a

*Authors to whom correspondence should be addressed.

source material at 900 °C.[39] It was observed from the previous studies that to obtain the hierarchical nanostructures, usually catalyst or additives with a high temperature and/or low pressure is required. Consequently, there is a need to develop a simple and effective method to grow these types of hierarchical nanostructures with a high quality and in a large quantity at low-temperature without the use of catalyst or additives. Moreover, the reported hierarchical nanostructures also exhibited a strong deep level emission in the room-temperature PL spectrum which is related to the structural defects and impurities of the corresponding structures. Thus, it is important to have good optical properties for the synthesized hierarchical nanostructures to utilize them for the fabrication of efficient nanooptoelectronic devices.

In this paper, we report the synthesis of hierarchical ZnO nanostructures composed of ZnO nanoneedles on silicon substrate via simple thermal evaporation process by using metallic zinc powder in the presence of oxygen without the use of any kind of metal catalysts of additives at 460 °C. Importantly, the as-grown hierarchical structures are exhibiting a strong near band edge emission and confirming the good optical properties and hence presenting themselves as effective candidates for the fabrication of various efficient optoelectronic nanodevices in the near future. In addition to this, due to the sharp and small tips of the as-grown nanoneedles in the hierarchical structures, these nanostructures can also be applied for the fabrication of field emission devices, sensors, electromechanical coupled devices, and etc. The obtained nanostructures were examined in terms of their structural and optical properties and finally a plausible growth mechanism has been proposed for the formation of these structures.

2. EXPERIMENTAL DETAILS

2.1. Growth of Hierarchical ZnO Nanostructures

The hierarchical ZnO nanostructures composed of nanoneedles were grown via the simple thermal evaporation process by using metallic zinc powder in the presence of oxygen without the use of any metal catalysts or additives. In a typical reaction process: commercially available 2.5 gram of high-purity metallic zinc powder (99.99%) was put into a quartz boat and placed at the centre of the quartz tube furnace. High purity nitrogen gas (99.999%) was also used as a carrier gas and to create the inert atmosphere during the whole reaction process. The substrates used in our experiments were bare silicon(111). Before experiments, the substrates were treated for 10 minutes with the buffer solution to remove the native oxide layer and keenly washed with de-ionized water, methanol, and acetone, sequentially and finally dried with inert gas (N_2). After loading the sample, the chamber pressure was down to 5 Torr using a rotary vacuum pump. For the experiment, the furnace temperature was ramped to desired growth temperature and high-purity oxygen (99.999%) and nitrogen gases were continuously introduced into the reaction chamber with the flow rates of 370 sccm (standard cubic centimeters per minute) and 150 sccm standard cubic centimeters per minute), respectively. The substrate temperature, placed 2.5 cm away from source material, was 460 °C. The reaction lasted in 20–100 minutes. After the growth process, the gray colored products were deposited onto the whole surface of the substrate. These deposited products on Si(111) substrate were examined in terms of their structural and optical properties.

2.2. Characterizations of Hierarchical ZnO Nanostructures

To determine the general morphologies of as-deposited hierarchical ZnO nanostructures, the synthesized products were examined by using field emission scanning electron microscopy (FESEM). The detailed structural characterization was done by the transmission electron microscope (TEM) and high-resolution TEM (HRTEM) containing the selected area electron diffraction (SAED) patterns. The crystallinity and crystal orientations of the as-grown hierarchical nanostructures were determined by using X-ray diffraction (XRD) pattern measured with Cu-Kα radiations ($\lambda = 1.54178$ Å) in the range of 25–80 ° at 40 kV. Raman scattering and room-temperature photoluminescence (PL) spectroscopy with the Ar^+ (513.4 nm) and He-Cd (325 nm) laser line as the exciton sources, respectively, were used to examine the optical properties of as-synthesized hierarchical ZnO nanostructures.

3. RESULTS AND DISCUSSION

The general morphologies of the as-deposited structures were examined by using field-emission scanning electron microscopy (FESEM) and shown in Figure 1. The low-magnification image of the grown hierarchical structures is shown in Figure 1(a) which clearly exhibits that the grown structures are hierarchical-shaped lying on the substrate surface and grown in very high-density onto a large area of the substrate. The typical diameters and lengths of hierarchical structures are about 1.5–2 μm and several tens of micrometers, respectively. The clear views of the as-grown hierarchical nanostructures are shown in Figures 1(b and c) which confirmed that the hierarchical structures are composed of thin nanoneedles, grown at the corners of the core ZnO wires/rods. Figures 1(d–f) exhibit the high-resolution and very clear images of ZnO nanoneedles grown in the hierarchical structures. The obtained ZnO nanoneedles show sharp tips and exhibiting a symmetrical and almost aligned arrangement at each corners of core ZnO wires/rods. The average lengths and diameters of each nanoneedle are 35 ± 10 nm and 550 ± 100 nm, respectively.

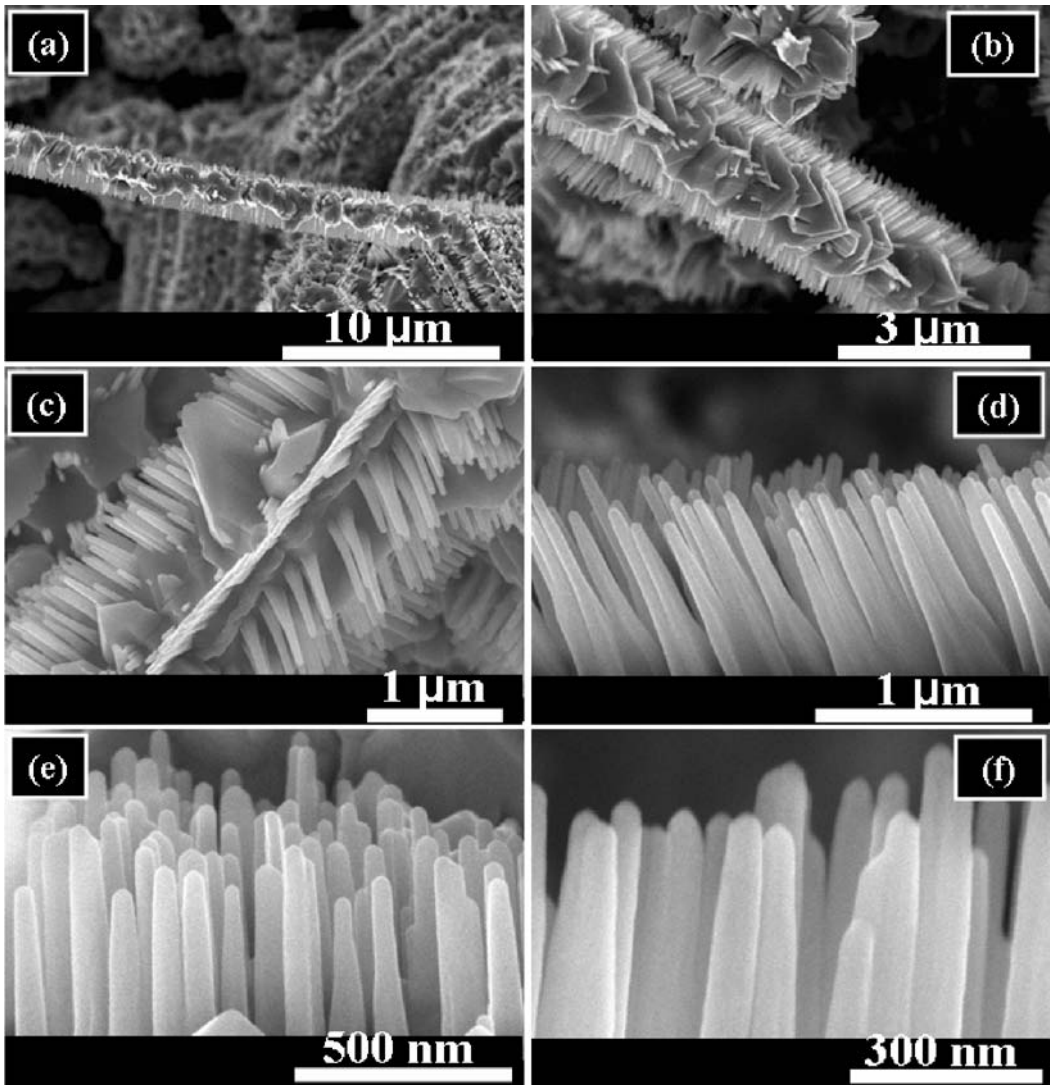

Fig. 1. (a)–(c) Low-magnification typical FESEM images of as-grown hierarchical ZnO structures; and (d)–(f) high-resolution FESEM images of ZnO nanoneedles grown in the hierarchical ZnO structures. These hierarchical structures are grown on silicon substrate at low-temperature of 460 °C using metallic zinc powder in the presence of oxygen by thermal evaporation process.

The crystallinity and phase identification of the as-grown hierarchical ZnO structures have been ascertained by X-ray diffraction (XRD) analysis measured with Cu-Kα radiation and shown in Figure 2. All the peaks in this pattern can be indexed to pure wurtzite hexagonal phase of bulk ZnO with the cell constants comparable to the already reported values (Joint Committee on Powder Diffraction Standards; JCPDS, Card No. 75-1526). The observed diffraction pattern revealed that the obtained hierarchical ZnO structures are single-crystalline with the wurtzite hexagonal phase. Moreover, no other peaks related to unreacted precursors and impurities are observed from the pattern, confirming that the grown products are pure ZnO. In addition to this, a peak at 34.2°, assigned as ZnO(0002), is the strongest as compared to other ZnO peaks obtained in the pattern confirming that the as-grown hierarchical ZnO structures are preferentially grown along the c-axis in (0001) direction. The detailed structural properties of the as-grown hierarchical ZnO structures was examined by using transmission electron microscopy (TEM) and high-resolution TEM (HRTEM) equipped with the selected area electron diffraction (SAED) pattern and shown in Figure 3.

Figure 3(a) shows the low-magnification TEM images of the ZnO nanoneedles grown in the hierarchical ZnO structures. This image is fully consistent with the FESEM observations and clearly exhibits that the grown nanoneedles have smooth and clean surfaces throughout their length and the diameters of root portion of the nanowires are more as compared to their tips. The diameters of the nanowires are gradually decreases with increasing the length and finally needle-shape is formed. The typical diameter of their tips and roots are in the range of 15–25 nm and 30–40 nm, respectively. The corresponding selected area electron diffraction (SAED) pattern

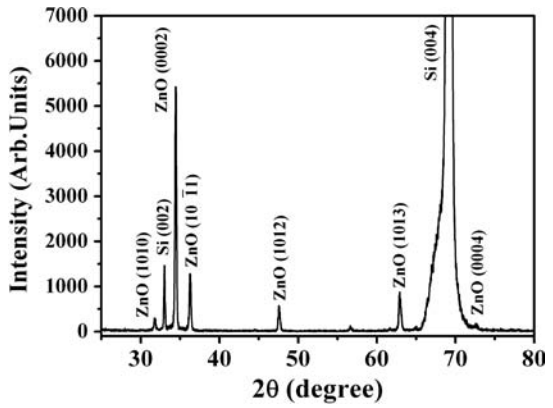

Fig. 2. Typical X-ray diffraction pattern for the as-synthesized hierarchical ZnO structures grown onto the silicon substrate by thermal evaporation process at 460 °C.

(inset (a)) of the subsequent nanoneedles shown in (a) demonstrates that the grown products are single-crystalline and grown along the c-axis direction in preference.

Figure 3(b) reveals the high-resolution TEM (HRTEM) image of the corresponding nanoneedle shown in Figure 3(a). The well-resolved interference lattice fringes of about 0.52 nm have been observed which is an excellent agreement with the lattice constant of single crystalline ZnO and indicates that the deposited materials have wurtzite hexagonal structure and grown along the [0001] direction. The corresponding SAED pattern (inset 3(b)), projected along the $[2\bar{1}\bar{1}0]$ zone axis reveals a well defined, ordered diffraction pattern indicating very high crystallinity (single crystal) with the c-axis growth direction of the grown ZnO needles. The SAED patterns are fully consistent with HRTEM and XRD observations.

Since no metal catalyst or any other type of additive was used during the synthesis of hierarchical ZnO structures and after the growth no metal particles or any other type of impurity was observed on the tips of the grown products, hence one can confirmed that the growth process of hierarchical structures does not follow the vapor-liquid-solid (VLS)[18, 29] mechanism but govern under the vapor-solid (VS) mechanism.[3, 4, 7, 8, 19, 20] Actually, the growth of hierarchical ZnO structures follows the two step process. In which the first step involved the growth of core ZnO wires/rods while the nanoneedles were formed around the core wires/rods in the next step. Therefore, the possible growth process of the hierarchical ZnO structures can be understood as follows: primarily, during the heating process, the source material metallic zinc powder (melting point of zinc = 419.6 °C) was melted due to higher reaction temperature and generated the zinc vapors which were transported from the source boat to the substrates by the nitrogen carrier gas. As can be seen from the FESEM images that the core ZnO rods are formed by the accumulation of many small ZnO crystals (Figs. 1(b and c)), hence we believe that during growth at first step, the growth of ZnO crystals occurs which later jointed each other in such a manner that they made a rod like morphologies. These rods-like morphologies serve as core structures for the growth of final hierarchical morphologies. At certain reaction time, the growth of rods-like morphologies made by ZnO crystals stopped and the outer surfaces of wires/rods get nucleated. With prolonged reaction, the initially formed ZnO nuclei, grown at the outer surfaces of the cored wires/rods, develop to sizes larger than the critical sizes and finally lead the formation of needle-like structures via the self-catalytic growth process and

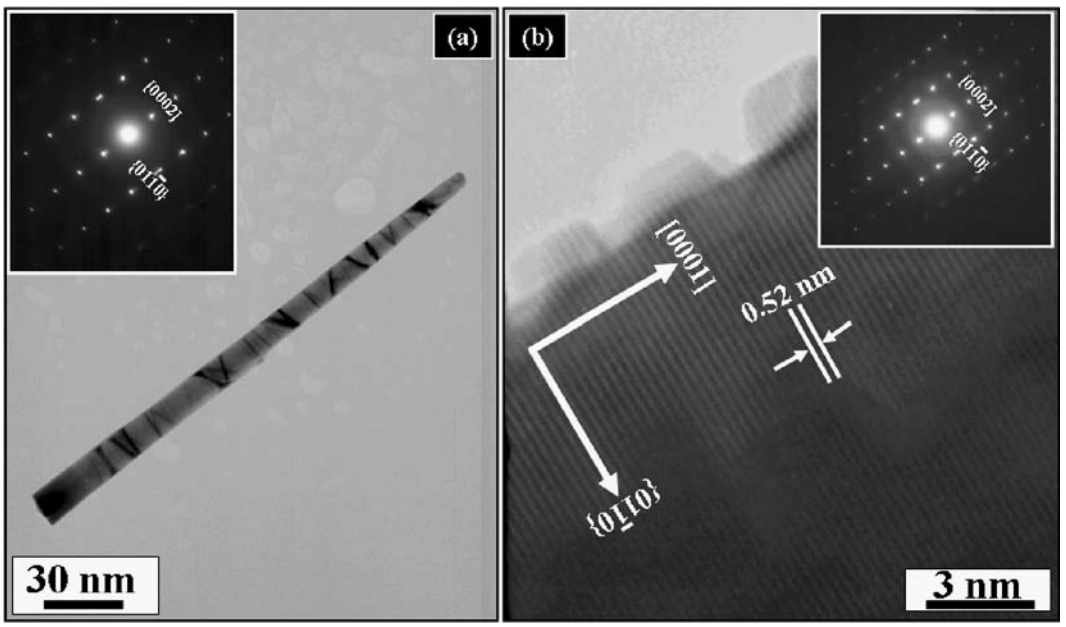

Fig. 3. (a) Low-magnification and (b) high-resolution TEM images of as-grown ZnO nanoneedles grown in the hierarchical ZnO structures. Inset (a) and (b) exhibit the corresponding SAED patterns of the subsequent structures.

RESEARCH ARTICLE

finally hierarchical structures can be obtained.[20] In addition to this, structurally, the wurtzite hexagonal ZnO crystal is composed of O^{2-} and Zn^{2+} ions, arranged in a tetrahedral manner and stacked alternatively along the c-axis direction. Due to the polar nature of ZnO crystals, it has oppositely charged ions, i.e., positively charged Zn–(0001) and negatively charged O–(0001) polar surfaces which result the net dipole moment and divergence in the surface energy. It is reported that the growth of ZnO crystals is fastest in the Zn-terminated (0001) surfaces, due to its self-catalytic property, as compared to any other growth facets.[20, 31] Interestingly, it was observed that the grown nanoneedles at the outer surfaces of the core ZnO wires/rods follow the typical and ideal growth habit of ZnO crystals and exhibit a growth along the [0001] direction. This fact was also confirmed by the HRTEM and SAED pattern (Figs. 2 and 3).

Due to sensitivity of Raman-scattering to crystallization, structural disorders and defects in nanostructures, Raman-scattering studies have been performed for the as-grown hierarchical ZnO structures and shown in Figure 4. With a wurtzite hexagonal phase, the polar ZnO belongs to the C_{6V}^4 space group. According to the group theory, near the centre of Brillouin zone there are following optic modes: $A_1 + 2B_1 + E_1 + 2E_2$. In these optic modes, the A_1, E_1 and E_2 modes are Raman active while A_1 and E_1 are Raman and infra-red active both. Moreover, the A_1 and E_1 are split into two optical components: longitudinal (LO) and transverse (TO).[40] Figure 4 exhibits the typical Raman-scattering spectrum for the as-grown hierarchical ZnO structures. As can be seen from the spectrum that a sharp and dominated peak at 521 cm^{-1} was observed which is related with the silicon substrate. In addition to this, one another sharp peak at 437 cm^{-1} was appeared which can be assigned as optical phonon E_2 mode, a characteristic peak for the wurtzite lattice.[3] Two very small peaks positioned at 331 cm^{-1} and 378 cm^{-1} assigned to be as E_{2H}–E_{2L} (multi phonon) and A_{1T} modes, respectively were also observed in the spectrum.[3] Interestingly, no peak for the E_{1L} mode was found in the spectrum. Generally, it is believed that the appearance of E_{1L} mode in the Raman-scattering spectrum is related with the presence of defects during the formation into the crystal lattices of ZnO such as zinc interstitials and oxygen vacancies.[30] As the grown hierarchical structures are exhibiting only a sharp and strong optical phonon E_2 mode and no E_{1L} mode was observed from the spectrum, hence one can conclude that the as-grown hierarchical ZnO structures are highly crystalline with the wurtzite hexagonal phase and containing no or very less structural defects.

The room-temperature photoluminescence (PL) measurements were performed to know the optical properties of the as-synthesized products. Figure 5 shows the typical room-temperature PL spectrum of the as-grown hierarchical ZnO structures. A strong, sharp and dominated band at 380 nm in the UV region and a very weak, suppressed or almost negligible band in the range of 530–650 nm in the visible regions have been observed. The UV emission is also called as the near band edge emission and originated due to the free-exciton recombination while the visible emission known to be as deep level emission generated by the impurities and structural defects such as oxygen vacancies and Zn interstitials, etc. in the deposited products.[3, 41] It is also reported that the crystal-quality of the deposited ZnO structure have strong influence in the appearance of high UV emission and therefore betterment in the crystal quality (less structural defects and impurities such as oxygen vacancies and zinc interstitials) may enhance the intensity of UV emission as compared to the visible emission.[3, 41] Interestingly, in our synthesized hierarchical ZnO structures, the UV emission is dominated over the visible emission which confirmed that the grown products have good crystal quality with very few structural defects and impurities and are exhibiting an excellent optical properties. Due to good UV-optical properties of as-grown hierarchical ZnO structures, these structures can

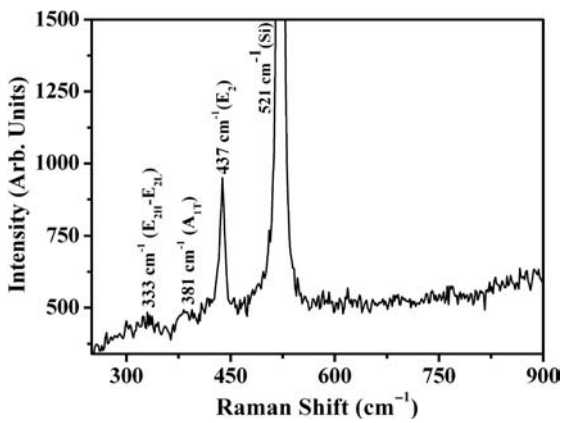

Fig. 4. Typical Raman-scattering spectrum of the as-synthesized hierarchical ZnO structures grown onto the silicon substrate by thermal evaporation process at 460 °C.

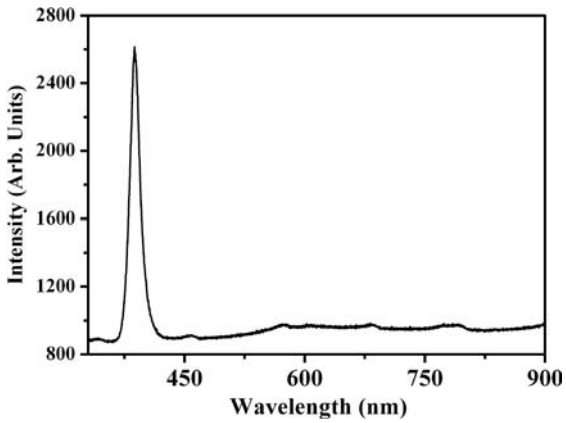

Fig. 5. Room-temperature photoluminescence (PL) spectrum of the as-synthesized hierarchical ZnO structures grown onto the silicon substrate by thermal evaporation process at 460 °C.

be effectively used in the fabrication of efficient UV-based optoelectronic nanodevices in near future.

4. CONCLUSION

Hierarchical ZnO nanostructures composed of ZnO nanoneedles were grown via thermal evaporation by using metallic zinc powder in the presence of oxygen. The detailed structural studies of the as-grown structures revealed that the synthesized products are single-crystalline with the wurtzite hexagonal phase and preferentially grown along the c-axis direction. Presence of a sharp and strong optical phonon E_2 mode at 437 cm^{-1} reveals the single-crystallinity and wurtzite hexagonal phase for the as-grown ZnO structures. A strong UV emission at 380 nm has been observed in the room-temperature PL spectrum which confirmed the excellent optical properties of as-synthesized hierarchical ZnO structures. Due to good optical properties, the as-grown hierarchical ZnO structures can be effectively used in the fabrication of efficient UV-based optoelectronic nanodevices in near future.

Acknowledgment: This work was supported in part by the Brain Korea 21 project in 2007 and the Korea Research Foundation grant (KRF-2005-005-J07502) (MOEHRD). KBSI, Jeonju branch and CURF, CBNU is also acknowledged.

RESEARCH ARTICLE

References and Notes

1. R. F. Service, *Science* 276, 895 (**1997**).
2. Y. R. Ryu, S. Zhu, J. D. Budai, H. R. Chandrasekhar, P. F. Miceli, and H. W. White, *J. Appl. Phys.* 88, 201 (**2000**).
3. A. Umar, B. Karunagaran, E.-K. Suh, and Y. B. Hahn, *Nanotechnology* 17, 4072 (**2006**).
4. A. Umar, B. K. Kim, J. J. Kim, and Y. B. Hahn, *Nanotechnology* 18, 175606 (**2007**).
5. M. H. Huang, S. Mao, H. Feick, H. Yan, Y. Wu, H. Kind, E. Weber, R. Russo, and P. Yang, *Science* 292, 1897 (**2001**).
6. M. Snure and A. Tiwari, *J. Nanosci. Nanotechnol.* 7, 481 (**2007**).
7. A. Umar, S. H. Kim, J. H. Kim, Y. K. Park, and Y. B. Hahn, *J. Nanosci. Nanotechnol.* 7, 4421 (**2007**).
8. A. Umar, S. H. Kim, J. H. Kim, and Y. B. Hahn, *J. Nanosci. Nanotechnol.* 7, 4522 (**2007**).
9. J. Q. Xu, Q. Y. Pan, Y. A. Shun, and Z. Z. Tian, *Sensors and actuators B; Chem.* 66, 277 (**2000**).
10. X. Wen, Y. Fang, Q. Pang, C. Yang, J. Wang, W. Ge, K. S. Wong, and S. Yang, *J. Phys. Chem. B* 109, 15303 (**2005**).
11. K. Keis, L. Vayssieres, S. Lindquist, and A. Hagfeldt, *Nanostruct. Mater.* 12, 487 (**1999**).
12. M. N. Jung, S. Y. Ha, H. S. Kim, H. J. Ko, H. Ko, W. H. Lee, D. C. Oh, Y. Murakami, T. Yao, and J. H. Chang, *J. Nanosci. Nanotechnol.* 6, 3628 (**2006**).
13. K. Hara, T. Horiguchi, T. Kinoshita, K. Sayama, H. Sugihara, and H. Arakawa, *Sol. Energy Mater. Sol. Cells* 64, 115 (**2000**).
14. H. Yumoto, T. Inoue, S. J. Li, T. Sako, and K. Nishiyama, *Thin Solid Films* 345, 38 (**1999**).
15. A. Kuoni, R. Holzherr, M. Boillat, and N. F. de Rooij, *J. Micromech. Microeng.* 13, S103 (**2003**).
16. Z.-G. Chen, F. Li, G. Liu, Y. Tang, H. Cong, G. Q. Lu, and H.-M. Cheng, *J. Nanosci. Nanotechnol.* 6, 704 (**2006**).
17. L. Jiang, X. Feng, J. Zhai, M. Jin, Y. Song, and D. Zhu, *J. Nanosci. Nanotechnol.* 6, 1830 (**2006**).
18. Z. L. Wang, *J. Nanosci. Nanotechnol.* 8, 27 (**2008**).
19. A. Umar and Y. B. Hahn, *Nanotechnology* 17, 2174 (**2006**).
20. A. Umar and Y. B. Hahn, *Appl. Phys. Lett.* 88, 173120 (**2006**).
21. Y. H. Huang, Y. Zhang, L. Liu, S. S. Fan, Y. Wei, and J. He, *J. Nanosci. Nanotechnol.* 6, 787 (**2006**).
22. A. Sekar, S. H. Kim, A. Umar, and Y. B. Hahn, *J. Crystal Growth* 277, 471 (**2005**).
23. A. Umar, S. H. Kim, Y. S. Lee, K. S. Nahm, and Y. B. Hahn, *J. Crystal Growth* 282, 131 (**2005**).
24. A. Umar, S. Lee, Y. S. Lee, K. S. Nahm, and Y. B. Hahn, *J. Crystal Growth* 277, 479 (**2005**).
25. A. Umar, M. M. Rahman, S. H. Kim, and Y. B. Hahn, *Chem. Commun.* (**2007**), in press.
26. S. Angappane, N. S. John, and G. U. Kulkarni, *J. Nanosci. Nanotechnol.* 6, 101 (**2006**).
27. S. J. Pearton, B. S. Kang, B. P. Gila, D. P. Norton, O. Kryliouk, F. Ren, Y.-W. Heo, C.-Y. Chang, G.-C. Chi, W.-M. Wang, and L.-C. Chen, *J. Nanosci. Nanotechnol.* 8, 99 (**2008**).
28. S. L. Mensah, A. Prasad, J. Wang, and Y. K. Yap, *J. Nanosci. Nanotechnol.* 8, 233 (**2008**).
29. W. L. Hughes and Z. L. Wang, *Appl. Phys. Lett.* 82, 2886 (**2003**).
30. B. P. Zhang, N. T. Binh, K. Wakatsuki, Y. Segawa, Y. Yamada, N. Usami, and H. Koinuma, *Appl. Phys. Lett.* 84, 4098 (**2004**).
31. W. L. Hughes and Z. L. Wang, *J. Am. Chem. Soc.* 126, 6703 (**2004**).
32. P. X. Gao and Z. L. Wang, *J. Appl. Phys.* 97, 44304 (**2005**).
33. A. Umar, S. Lee, Y. H. Im, and Y. B. Hahn, *Nanotechnology* 16, 2462 (**2005**).
34. G. Shen, Y. Bando, B. Liu, D. Golberg, and C. J. Lee, *Adv. Func. Mater.* 16, 410 (**2006**).
35. J. Y. Lao, J. G. Wen, and Z. F. Ren, *Nano Lett.* 2, 1287 (**2002**).
36. J. Y. Lao, J. Y. Huang, D. Z. Wang, and Z. F. Ren, *Nano Lett.* 3, 235 (**2003**).
37. J. Y. Lao, J. Y. Huang, D. Z. Wang, and Z. F. Ren, *J. Mater. Chem.* 14, 770 (**2004**).
38. P. X. Gao and Z. L. Wang, *Appl. Phys. Lett.* 84, 2883 (**2004**).
39. G. Shen, Y. Bando, and C.-J. Lee, *J. Phys. Chem. B* 109, 10779 (**2005**).
40. J. M. Calleja and M. Cardona, *Phys. Rev. B* 16, 3753 (**1977**).
41. D. M. Bagnall, Y. F. Chen, Z. Zhu, T. Yao, S. Koyama, M. Y. Shen, and T. Goto, *Appl. Phys. Lett.* 73, 1038 (**1998**).

Received: 14 February 2008. Revised/Accepted: 23 February 2008.